Hindawi Publishing Corporation
Journal of Biomedicine and Biotechnology
Volume 2011, Article ID 386384, 10 pages
doi:10.1155/2011/386384

Research Article

Both Basic and Acidic Amino Acid Residues of $IpTx_a$ Are Involved in Triggering Substate of RyR1

In Ra Seo,[1,2] Dae Eun Kang,[1,2] Dong Woo Song,[1,2] and Do Han Kim[1,2]

[1] *Systems Biology Research Center, Gwangju Institute of Science and Technology (GIST), Gwangju 500-712, Republic of Korea*
[2] *School of Life Sciences, Gwangju Institute of Science and Technology (GIST), 1 Oryong-dong, Buk-gu, Gwangju 500-712, Republic of Korea*

Correspondence should be addressed to Do Han Kim, dhkim@gist.ac.kr

Received 1 June 2011; Revised 5 August 2011; Accepted 10 August 2011

Academic Editor: Aikaterini Kontrogianni-Konstantopoulos

Imperatoxin A ($IpTx_a$) is known to modify the gating of skeletal ryanodine receptor (RyR1). In this paper, the ability of charged aa residues of $IpTx_a$ to induce substate of native RyR1 in HSR was examined. Our results show that the basic residues (e.g., Lys^{19}, Lys^{20}, Lys^{22}, Arg^{23}, and Arg^{24}) are important for producing substate of RyR1. In addition, other basic residues (e.g., Lys^{30}, Arg^{31}, and Arg^{33}) near the C-terminus and some acidic residues (e.g., Glu^{29}, Asp^{13}, and Asp^{2}) are also involved in the generation of substate. Residues such as Lys^{8} and Thr^{26} may be involved in the self-regulation of substate of RyR1, since alanine substitution of the aa residues led to a drastic conversion to the substate. The modifications of the channel gating by the wild-type and mutant toxins were similar in purified RyR1. Taken together, the specific charge distributions on the surface of $IpTx_a$ are essential for regulation of the channel gating of RyR1.

1. Introduction

In striated muscles, depolarization of the cell surface membranes leads to activation of ryanodine receptors (RyRs) in the junctional sarcoplasmic reticulum (SR) [1–5]. A number of endogenous RyR modulators such as calmodulin, FK506-binding proteins, calsequestrin, triadin, and HRC have been identified [6–8]. Exogenous modulators of RyRs such as toxins and peptides have also been reported [9, 10].

Imperatoxin A ($IpTx_a$) from the African scorpion *Pandinus* imperator is a high-affinity modulator of skeletal RyR (RyR1). It greatly increases open probability (P_o) and [^{3}H]ryanodine binding to RyR1 at nanomolar concentration [11, 12]. Moreover, binding of $IpTx_a$ to RyRs reconstituted in planar lipid bilayers generates marked occurrence of long-lasting openings in subconductance state (substate) [13]. Confocal imaging of skeletal muscle fibers to monitor $IpTx_a$-induced Ca^{2+} sparks demonstrate that the toxin induces long-duration and low-amplitude local Ca^{2+} release consistent with the observation of the prolonged substate in the presence of $IpTx_a$ [14]. Another structurally related scorpion toxin, maurocalcine (MCa), and one specific small fragment of II-III loop region of skeletal DHPR (Peptide A) also bind to RyR1 and modify channel activity [15–18]. MCa also strongly enhances [^{3}H]ryanodine binding to RyR1 and induces long-lasting substate with the current amplitude of 48% of the full conductance [16, 18]. Peptide A could bind to RyR1 and could either activate or inhibit the activity of RyR1. It could also induce the long-lasing substate [15, 17, 19].

A comparison of the amino acid (aa) sequences of these RyR1-modifing probes shows a common basic aa domain and the C-terminal hydroxyl-containing side chain. The aa sequences may also contribute to the essential structure for activating RyR1 [15, 16]. Especially, a cluster of positively charged aa residues on the surface of the peptide A is critical for activation of RyR1 [19, 20]. The mutations of the specific basic residues of MCa and $IpTx_a$ have failed to induce long-lasting substate and to potentiate [^{3}H]ryanodine binding [20, 21]. To date, the ability of a single aa residue of $IpTx_a$ to control the substate of RyR1 is not fully understood. Recently we have found that several basic aa residues of $IpTx_a$ (e.g., Lys^{19}, Arg^{23}, and Arg^{33}) are necessary for increasing open probability and inducing substate in rabbit skeletal RyR1 [22].

In the present study, to evaluate the roles of the charged aa residues of $IpTx_a$ in modifying the RyR1 gating, synthetic wild-type and alanine-scanning mutants of $IpTx_a$ were tested on planar lipid bilayer-incorporated RyR1. The basic aa mutants (e.g., K19A, K20A, K22A, R23A, and R24A) resulted in a significant loss of production of substate in RyR1, consistent with the previous suggestion that the critical basic domain of toxin determines its binding to the channel [15, 16, 22]. The effective domain encompassing these basic residues involved in producing substate is structurally conserved with both MCa and Peptide A [19, 23]. This suggests a common role of the highly clustered positive charges for their action on RyR1 channel gating. The mutations of some acidic residues (e.g., Asp^2, Asp^{13}, and Glu^{29}) and basic residues within C-terminal region of $IpTx_a$ (e.g., Lys^{30}, Arg^{31}, and Arg^{33}) also led to a significant inhibition on the gating. When Lys^8 and Thr^{26} were replaced by alanine, the substate was predominant indicating that these two residues are essential for the functions of the toxin. In addition, the effects of the wild-type and mutant toxins on the gating behavior of RyR1 are strikingly similar when the native RyR1 in SR and the purified RyR1 are used for the incorporation into bilayers, suggesting that generation of the substate is due to a direct binding of the toxin to RyR1.

2. Materials and Methods

2.1. Materials. Porcine brain phosphatidylethanolamine and phosphatidylserine were purchased from Avanti Polar Lipids, Inc. All other reagents were from Sigma.

2.2. Chemical Synthesis of Wild-Type and Mutant $IpTx_a$ Peptides. The peptide synthesis was conducted by a peptide synthesizer (Applied Biosystems model 433A). The linear precursors of wild-type and mutant $IpTx_a$ were synthesized by solid-phase Fmoc chemistry starting from Fmoc-Arg (2,2,5,7,8-pentamethylchroman-6-sulphonyl)-Alko or Fmoc-Ala-Alko resin using a variety of blocking groups for amino acid protection. After cleavage by trifluoroacetic acid, crude linear peptides were extracted with 2 M ethanoic acid, diluted to final peptide concentration of 25 μM in a solution of 1 M ammonium acetate and 2.5 mM reduced/0.25 mM oxidized glutathione adjusted to pH 7.8 with aqueous NH_4OH, and stirred slowly at 4°C for 2-3 days. In the redox buffer system, oxidized glutathione acts as oxidase and assists in the formation of disulfide bonds whereas reduced glutathione functions as disulfide isomerase and facilitates formation of correct disulfide bonds by promoting rapid reshuffling of incorrect disulfide parings. A 10 : 1 mixture of reduced and oxidized glutathione was suggested to be an efficient redox buffer system for producing disulfide bonds in $IpTx_a$ [21]. The folding reactions were monitored by HPLC. The crude oxidized products were purified by successive chromatography with CM-cellulose CM-52 and preparative HPLC with C18 silica columns. The purity of all analogues were in the range of 60 to 95% as measured by analytical HPLC and MALDI-TOF-MS (matrix-assisted laser desorption ionization-time-of-flight MS) measurements (see Supplementary Figure 1 (in Supplementary material available online at doi: 10.1155/2011/386384)).

2.3. Preparation of Junctional SR Vesicles from Rabbit Skeletal Muscle. A heavy fraction of fragmented SR vesicles (HSR) containing junctional SR was prepared from rabbit fast-twitch back and leg muscles as described previously [24].

2.4. Planar Lipid Bilayers. Single-channel recordings of rabbit skeletal RyR1 incorporated into planar lipid bilayers were carried out as described previously [25–27]. Lipid bilayers, consisting of brain tissue phosphatidylethanolamine and phosphatidylserine (1 : 1) in decane (20 mg/mL) were formed across a hole of approximately 200 μm diameter. Thinning of the bilayer was monitored by bilayer capacitance. The basic composition of the *cis*/*trans* solution consisted of 300 mM cesium methanesulfonate, 10 mM Tris/Hepes (pH 7.2), 2 mM EGTA, and 1.998 mM $CaCl_2$ ($[Ca^{2+}]_{free}$ = 10 μM) [27]. $[Ca^{2+}]_{free}$ was calculated using the "Chelator" program (Theo Schoenmaker). Cs^+ was selected as the charge carrier to ensure precise control of free $[Ca^{2+}]$, to increase the channel conductance, and to avoid any contribution from potassium channels present in the SR membrane [12]. Chloride channels were inhibited by using the impermeant anion methanesulfonate [12]. Incorporation of ion channels was carried out as described by Miller and Racker [25] and confirmed by recording the characteristically high single-channel conductance of RyRs [27, 28]. The *trans* side was maintained at ground and the *cis* side was clamped at −30 mV relative to the ground. After addition of the $IpTx_a$ to the *cis* chamber, the single channel data were collected at −30 mV for 2–5 min. The channel activity was recorded on a DTR-1204 Digital Recorder (Biologic Science Instrument) and displayed on a Tektronix TDS 340A oscilloscope. Recordings were filtered with an 8-pole low-pass Bessel filter at 1 kHz and digitalized through a Digidata 1200 series interface (Axon Instruments). Data acquisition and analysis were done with the Axon Instruments software, pClamp v7.0.

Data were analyzed using the Hill equation described previously [12, 13, 15]:

$$P_{\text{substate}} = \frac{(P_{\text{substate, max}})}{\left[1 + (EC_{50}/[IpTx_a])^{nH}\right]} \text{ or}$$
$$P_o = \frac{(P_{o,\text{ max}})}{\left[1 + (EC_{50}/[IpTx_a])^{nH}\right]}, \quad (1)$$

where $(P_{o,\text{ max}})$ is the P_o observed at saturating concentrations of $IpTx_a$, EC_{50} is the $IpTx_a$ concentration for which 50% of $P_{o,\text{max}}$ is obtained and nH is the Hill coefficient. Also, $P_{\text{substate, max}}$ is the P_{substate} observed at saturating concentrations of $IpTx_a$, EC_{50} is the $IpTx_a$ concentration for which 50% of $P_{\text{substate, max}}$ is obtained, and nH is the Hill coefficient. The probability of full open state of the channel (P_o) was defined as the ratio of the time spent in the open state to the total time exclusive of time spent in the substate. The probability to obtain substate (P_{substate}) was calculated

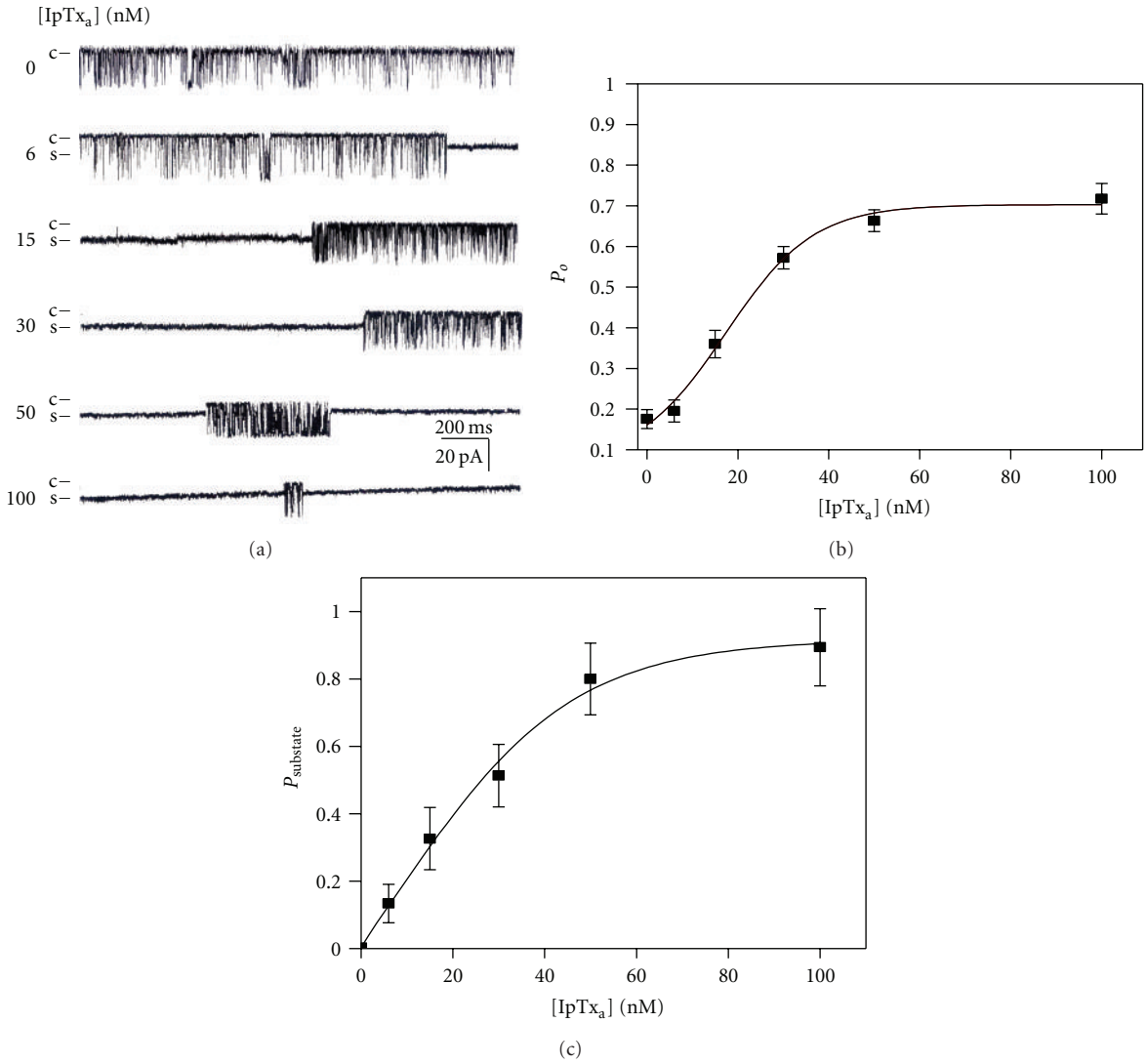

Figure 1: Properties of single channel gating in IpTx$_a$-modified native RyR1. (a) Channel current traces of a single skeletal RyR1 in planar lipid bilayers activated by various concentrations of IpTx$_a$. IpTx$_a$ at 6–100 nM (final) was added to the *cis* solution to activate the channel. Channel openings are shown as downward deflections. Channel activities were recorded at a holding potential of −30 mV. (b) A plot of P_o versus concentration of IpTx$_a$ to activate rabbit skeletal RyR1. Data points are means ± SE of ten experiments. (c) A plot of $P_{substate}$ versus IpTx$_a$ concentration for rabbit skeletal RyR1. Data points are means ± SE of 9 experiments.

as the time spent in the substate divided by a given total recording time. The durations of the substate were obtained by manual positioning of the cursors and constructing all point histograms. Mean duration of substate was measured by total substate time divided by total substate frequencies.

2.5. Statistical Analysis. Results are given as means ± SE. Significant differences were analyzed using Student's *t*-test. Differences were considered to be significant when $P < 0.05$. The fitting of the data to the graphs were carried out using the software, Origin v7.

3. Results

3.1. Effects of IpTx$_a$ on Single-Channel Gating Properties of RyR1. To examine how IpTx$_a$ modifies RyR1 activity, RyR1 in HSR incorporated in planar lipid bilayers was tested in the presence or absence of synthetic wild-type IpTx$_a$. The chamber solutions for both *cis* (cytosolic) and *trans* (luminal) sides included 300 mM cesium methanesulfonate and 10 mM Tris-Hepes (pH 7.2). 10 μM free Ca^{2+} was added to the *cis* side to activate the incorporated RyR1. After an addition of IpTx$_a$ to the *cis* chamber, the single channel gating properties were recorded at a holding potential of −30 mV for over 2 min at each toxin concentration. Figure 1(a) shows traces from continuous recordings in the absence and in the presence of 6, 15, 30, 50, and 100 nM IpTx$_a$. When the toxin concentration increased, the occurrence of substate of RyR1 was remarkably increased. To examine the effects of IpTx$_a$ on full open state, we calculated the probability to obtain the full open state (P_o) as the time spent in the open state divided by the total time exclusive

of the time spent in the substate. The time for recorded P_o was in the range of 30 s–2 min. Figure 1(b) shows a plot of P_o versus $IpTx_a$ concentration at 10 μM Ca^{2+}. The steady-state P_o was 0.18 ± 0.02 at 10 μM Ca^{2+}. When the concentration of $IpTx_a$ was increased in *cis* chamber, P_o increased markedly to 0.7, suggesting that the cytosolic $IpTx_a$ enhanced the channel activity by increasing open probability in a dose-dependent manner. Using the Hill equation (1) the parameters such as $P_{o,\max}$, EC_{50}, and Hill coefficient (nH) were calculated. The calculated $P_{o,\max}$ and EC_{50} for P_o were 0.72 ± 0.02 and 17.35 ± 4.67 nM, respectively. The Hill coefficient (nH) for P_o was 1.14. Application of $IpTx_a$ to the *trans* (SR lumen) side of chamber did not show any effect (data not shown), suggesting that increase of the full opening events of the RyR1 channel is due to interaction between the toxin and the cytosolic region of the channel.

In light of the evidence that $IpTx_a$ could induce substate both in cardiac and skeletal RyRs [13], the effects of synthetic $IpTx_a$ on the occurrence of substate were tested using native RyR1 in rabbit skeletal HSR. Figure 1(a) shows that an addition of $IpTx_a$ to the *cis* side of RyR1 channel could induce the substate. The probability to obtain substate ($P_{substate}$) increased, when the concentration of $IpTx_a$ increased from 6 to 100 nM in the *cis* chamber (Figure 1(c)). The calculated $P_{substate,\ max}$ and EC_{50} for $P_{substate}$ were 0.92 ± 0.06 and 23.27 ± 2.37 nM, respectively. The Hill coefficient (nH) for $P_{substate}$ was 1.24, suggesting that $IpTx_a$ and RyR1 do not have the cooperative bindings in the concentration range.

Table 1: Effects of the mutant $IpTx_a$ on $P_{substate}$ of native RyR1 in SR. $P_{substate,\ max}$ and EC_{50} for $P_{substate,\ max}$ were calculated using (1) as described in "Section 2." Values are means ± SE of 3–9 experiments. The average lengths of the substate events were determined at 30 nM concentration. Asterisks indicate significant differences from the wild-type toxin for each parameter (Student t-test, $P < 0.05$). ND: not determined.

	$P_{substate}$		Mean duration of substate (s)
	$P_{substate,\ max}$	EC_{50} (nM)	
Wild type	0.92 ± 0.06	23.27 ± 2.37	4.56 ± 0.42
K8A	0.97 ± 0.01	5.70 ± 2.86*	ND
T26A	0.98 ± 0.05	9.98 ± 1.92*	3.66 ± 0.40*
D15A	0.91 ± 0.05	21.47 ± 1.92	4.50 ± 0.51
R9A	0.75 ± 0.05*	19.91 ± 3.16	5.86 ± 0.52*
K11A	0.70 ± 0.07*	21.76 ± 3.49	4.35 ± 1.07
D13A	0.62 ± 0.07*	21.72 ± 7.92	2.76 ± 0.25*
K19A	0.43 ± 0.07*	21.84 ± 6.47	1.94 ± 0.43*
R31A	0.40 ± 0.03*	19.24 ± 4.65	3.42 ± 0.27*
D2A	0.38 ± 0.08*	28.63 ± 14.02	2.96 ± 0.60*
R23A	0.32 ± 0.09*	19.54 ± 9.36	2.50 ± 0.26*
R24A	0.26 ± 0.08*	26.03 ± 7.01	1.55 ± 0.94*
E29A	0.19 ± 0.03*	6.07 ± 4.28*	1.75 ± 0.29*
K30A	0.19 ± 0.02*	16.66 ± 2.86*	1.72 ± 0.39*
K20A	0.18 ± 0.05*	18.53 ± 8.17	3.64 ± 0.78*
R33A	0.14 ± 0.03*	16.03 ± 5.65*	1.97 ± 0.19*
K22A	0.12 ± 0.02*	18.49 ± 2.88	3.31 ± 0.15*

3.2. Effects of Alanine Scanning Mutants of $IpTx_a$ on RyR1. In the previous studies [21, 22], it was proposed that specific basic amino acid residues on the surface of $IpTx_a$ are required for the electrostatic interaction of the toxin with RyR1. Particularly, Gurrola et al. [15] suggested the structural domain composed of Lys^{19}-Arg^{24} followed by Thr^{26} is responsible for the $IpTx_a$-RyR1 binding. A possible molecular interaction between $IpTx_a$ and RyR1 was further investigated in the present study by producing various alanine scanning mutants at charged aa. We first tested the effects of $IpTx_a$ mutants on substate of RyR1 at a holding potential of –30 mV.

The single channel traces of RyR1 activated at 30 nM wild type or mutant $IpTx_a$ are shown in Figure 2(a). Ability of the different mutant toxins to induce substate of RyR1was further tested using different toxin concentrations. Interestingly, both K8A and T26A mutants displayed a significantly increased substate lifetime, indicating a negative role of these residues in modifying RyR1 gating. $P_{substae,\ max}$ of K8A or T26A reached almost to 1, and EC_{50} (nM) values were shifted from 23.27 ± 0.37 (wild type) to 5.70 ± 2.86 (K8A) or to 9.98 ± 1.92 (T26A; Figure 2(b) and Table 1). The mutations of the basic aa (Lys^{19}, Lys^{20}, Lys^{22}, Arg^{23}, Arg^{24}, Lys^{30}, Arg^{31}, and Arg^{33}) significantly reduced the probability to obtain substate ($P_{substate}$), compared with the wild-type toxin (Figure 2(b) and Table 1). The effect of D15A mutant was similar to that of wild-type toxin, suggesting no major involvement of Asp^{15} in the binding between the toxin and RyR1. On the other hand, the substitutions of some acidic aa such as Asp^2, Asp^{13}, and Glu^{29} by alanine alter the probability to obtain substate significantly (Figure 2 and Table 1). These results suggest that the charged aa distributed on the surface of $IpTx_a$ contribute to the stimulatory action of the toxin and to the interaction between $IpTx_a$ and RyR1.

3.3. Mean Duration of $IpTx_a$-Induced Substate. To investigate the causes for the decreased $P_{substate}$ by the mutant toxins, the average length of substate at 30 nM wild type or mutant of $IpTx_a$ was calculated as total substate time divided by the toral frequencies of substate. The recording time in each concentration was 2 min. Despite the marked increase in $P_{substate}$ as $IpTx_a$ was increased from 6 nM to 100 nM, the mean duration of the $IpTx_a$ induced-substate of RyR1 appeared to be similar at different [$IpTx_a$] (Figure 4). The average mean duration of substate of the mutants (D2A, D13A, K19A, K22A, R23A, R24A, E29A, K30A, and R33A) was significantly less than that of wild-type $IpTx_a$ (Table 1). Some mutants (K19A, R24A, E29A, and K30A) showed more marked reduction in mean duration of substate (<2 s). The decreased mean duration of substate in the mutant toxins is due probably to the loss of their ability to induce long-lasting substate.

3.4. Effects of $IpTx_a$ on Purified RyR1. To determine whether the activation of native RyR1 in SR by $IpTx_a$ was due to a direct activation of RyR1 or due to an indirect activation through other proteins associated to RyR1, we added $IpTx_a$

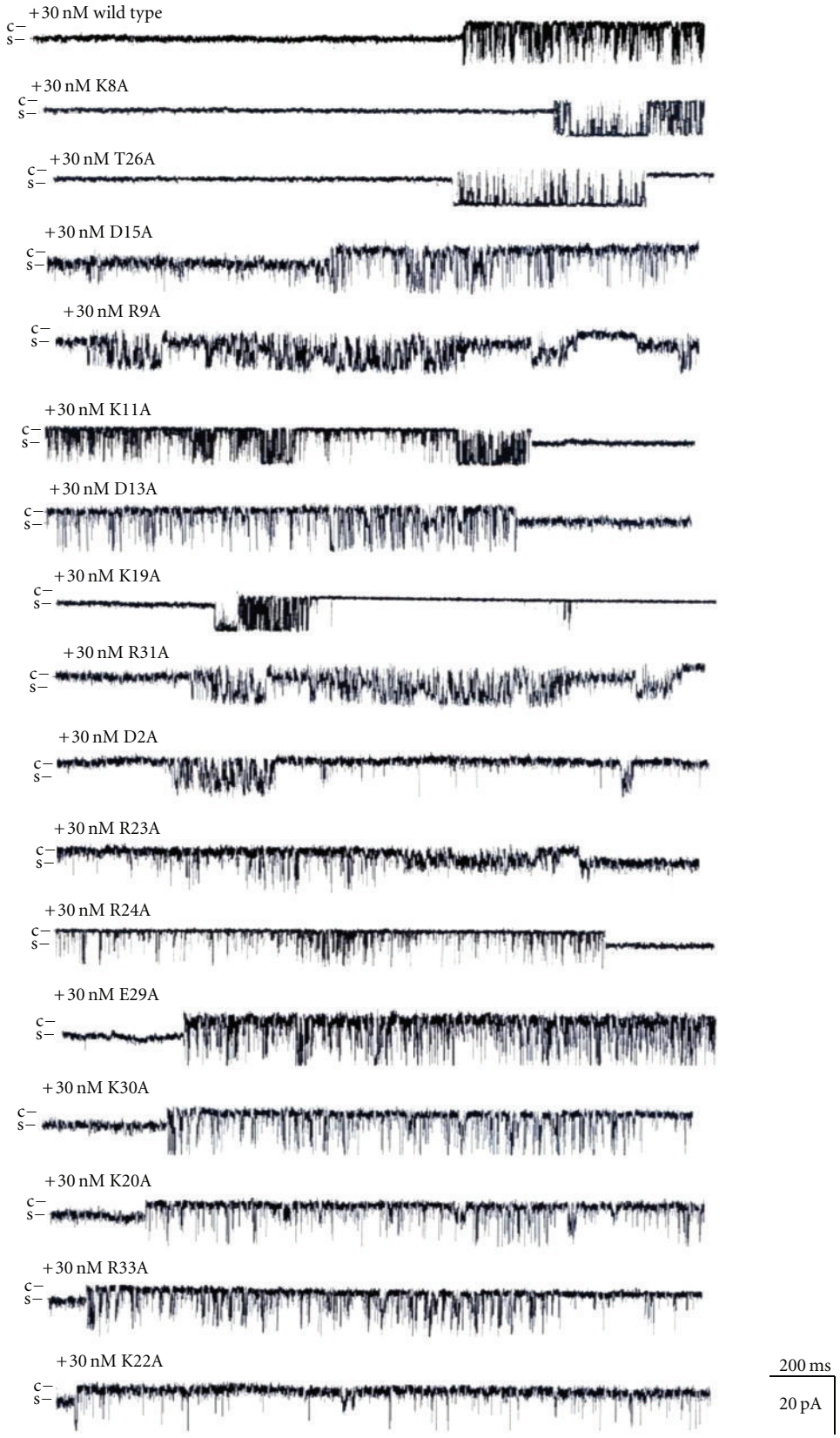

(a)

Figure 2: Continued.

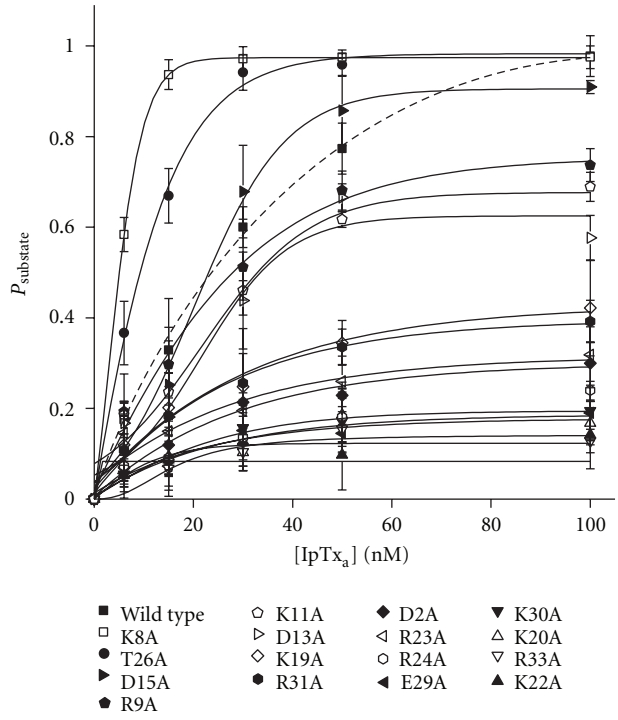

(b)

Figure 2: Single channel current traces of RyR1 modified by various alanine scanning IpTx$_a$ mutants. (a) Single channel current traces of skeletal RyR1 activated in the presence of 30 nM wild-type or various mutant IpTx$_a$ (*cis* side) at −30 mV holding potential. Single channel opening is shown as a downward deflection. (b) The plots of $P_{substate}$ of RyR1 versus concentration of IpTx$_a$ are shown. The data points are means ± SE from 3–5 independent experiments.

to purified RyR1 incorporated into planar lipid bilayers (Figure 3(a)). 30 nM IpTx$_a$ increased $P_{substate}$ both in native and purified RyR1 in a similar extent (Figures 1 and 3). Figure 4 shows that the mean durations of substate of purified RyR1 are similar to native RyR1 at the tested concentration range, suggesting that the response of RyR1 to IpTx$_a$ was not mediated by other RyR1-associated proteins. Purity of RyR1 at the final purification step was verified by Coomassie blue staining (Supplementary Figure 2).

3.5. Effects of IpTx$_a$ Mutants on Purified RyR1. We further tested the effects of mutant IpTx$_a$ (K8A, K30A, R31A, or R33A) on $P_{substate}$ of purified RyR1. Channel activity was monitored for 2 min in the presence of 6 to 100 nM mutant toxins (Figure 5(a)). The plots of $P_{substate}$ versus [IpTx$_a$] showed that the mutant toxins (K30A, R31A, and R33A) led to much smaller $P_{substate}$ (0.16 ± 0.05, 0.15 ± 0.02, and 0.18 ± 0.06, resp.) than that of wild-type IpTx$_a$(0.86 ± 0.05) without a significant change of EC_{50} (Figure 5(b) and Table 2). K8A led to similar $P_{substate,\,max}$ (0.85 ± 0.02) to wild-type toxin (Figure 5(b)). K30A and R33A produced less than 2 s of mean duration of substate (Table 2).

4. Discussion

4.1. Effects of IpTx$_a$ Mutants on Substate of RyR1. The highly positive charges of the basic residues of IpTx$_a$ could contribute to the formation of its functional surface area having uniquely oriented charge distribution [15, 19, 21–23]. In the present study we tested the hypothesis that electrostatic force mediates the IpTx$_a$-RyR1 interaction by studying the effects of alanine scanning mutations of charged aa residues in IpTx$_a$ on RyR1 functions.

Single point mutations of charged residues in IpTx$_a$ generally affected the probability of occurring substate ($P_{substate}$) in RyR1 (Figure 2 and Table 1). Previously, it was shown that mutations in a cluster of basic residues (Lys^{19}-Arg^{24}) decreased the ability of the toxin to activate [^{3}H]ryanodine binding to RyR1 [15, 21]. The recombinant mutant toxins (e.g., K19A, R23A, and R24A) were less effective to increase open probability (P_o) and to induce substate of the channel [22]. Our present results demonstrate that a cluster of the basic residues 19–24 is necessary for inducing substate of RyR1, confirming the functional importance of the clustered basic residues. In addition, replacing other basic residues located in C-terminal region of IpTx$_a$ with alanine (e.g., K30A, R31A, and R33A) also reduced the effects of the toxin on channel modification (Figure 2(b)). As described previously, the C-terminal basic residues (Lys^{22}, Arg^{23}, and Arg^{24}) are aligned in the central domain of IpTx$_a$ and possibly are responsible for activating RyR1 [21]. Our present findings agree with the previous suggestion that the positively charged region within the C-terminus is involved in the interaction with RyR1.

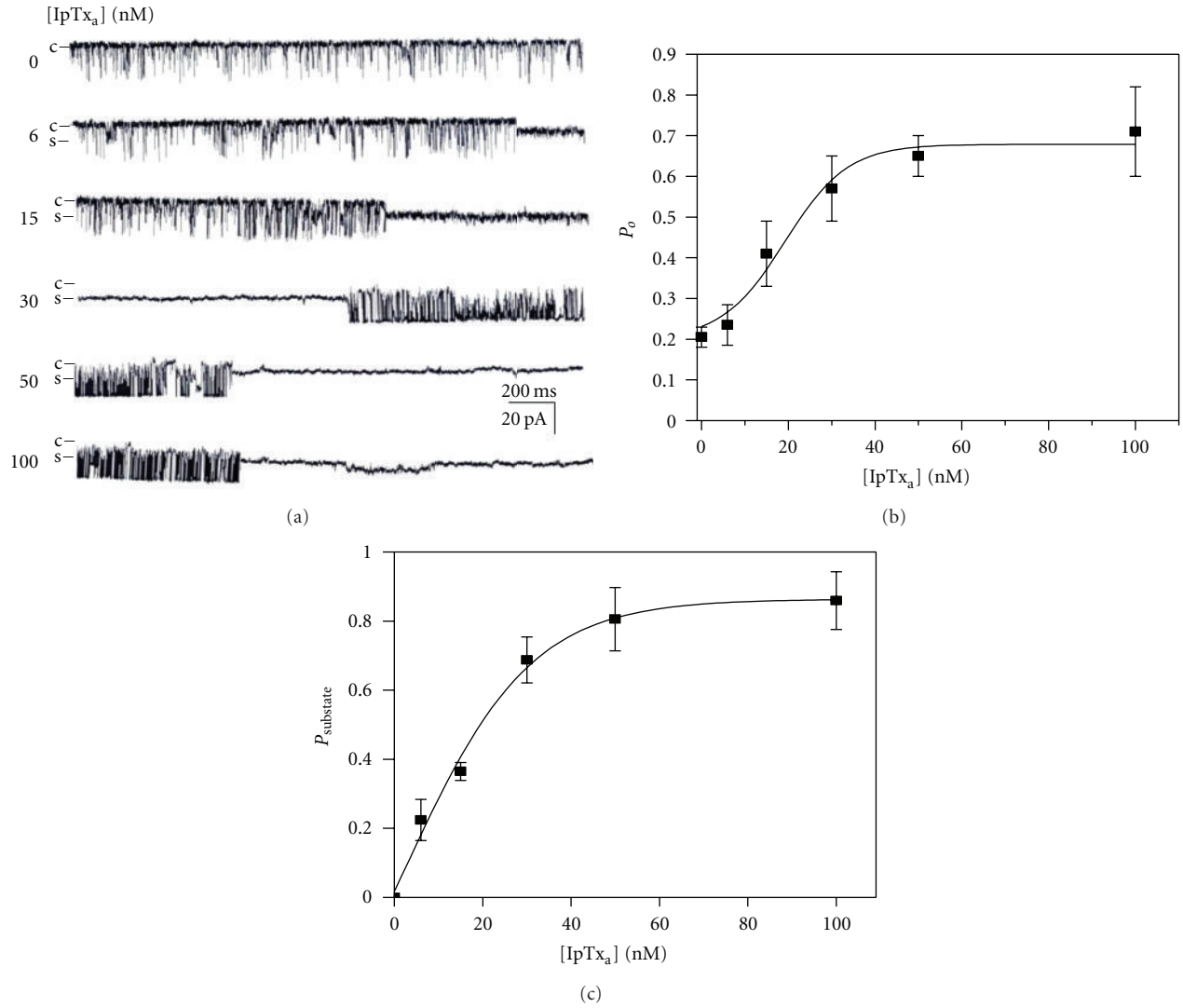

FIGURE 3: Effects of IpTx$_a$ on purified rabbit RyR1 incorporated in planar lipid bilayers. (a) Single channel activity of purified RyR1 incorporated in planar lipid bilayers at 10 μM Ca^{2+} with or without IpTx$_a$ (6–100 nM) was recorded. Single channel currents are shown as downward deflections from the closed level (indicated by c). The holding potential was −30 mV. (b) The plot of P_o of purified RyR1 versus various concentrations of IpTx$_a$ is shown. (c) The plot of $P_{substate}$ of purified RyR1 versus various concentrations of IpTx$_a$ is shown. The results are shown as the means ± SE for 7 experiments.

K8A and T26A, the two mutated analogs of IpTx$_a$, showed dramatically decreased EC_{50} of $P_{substate}$ compared to that of wild-type toxin, indicating higher binding affinity to RyR1 (Figures 2(b) and 5(b)). Although the ability of K8A to increase the substate lifetime of RyR1 was previously studied using recombinant IpTx$_a$ mutant [22], the effect of K8A on [^{3}H]ryanodine binding to RyR1 is controversial [15, 21]. T26A mutant was reported to reduce toxin-activated ryanodine binding to RyR1 [15]. The inconsistency between occurrence of substate and ryanodine binding to RyR1 affected by K8A or T26A suggests multiple independent actions of IpTx$_a$ on different modes of channel gating. In fact, Dulhunty et al. [17] proposed an existence of multiple toxin binding sites within RyR1 including the transient activation site and substate site [17].

4.2. The Effects of IpTx$_a$ and Peptide A on RyR1 Gating. Marked functional similarity of the three peptides, IpTx$_a$, MCa, and Peptide A has been proposed on the basis of their primary structural homology of a specific domain consisting of basic amino acids (Lys^{19}-Arg^{23} of IpTx$_a$ or MCa, and Arg^{681}-Lys^{685} of Peptide A) [15, 17, 18, 23, 29]. Stretches of these positively charged residues tend to adopt different secondary structures such as α-helical structure for Peptide A and β-sheet structure for IpTx$_a$ and MCa. However, their orientation on the surface of the peptides could be similar [19, 21]. Peptide A was shown to share the common binding site on RyR1 with IpTx$_a$ and MCa and mimicked the toxin effects on RyR1 gating [15, 23, 29]. However, evidence for noncompetitive binding of MCa and peptide

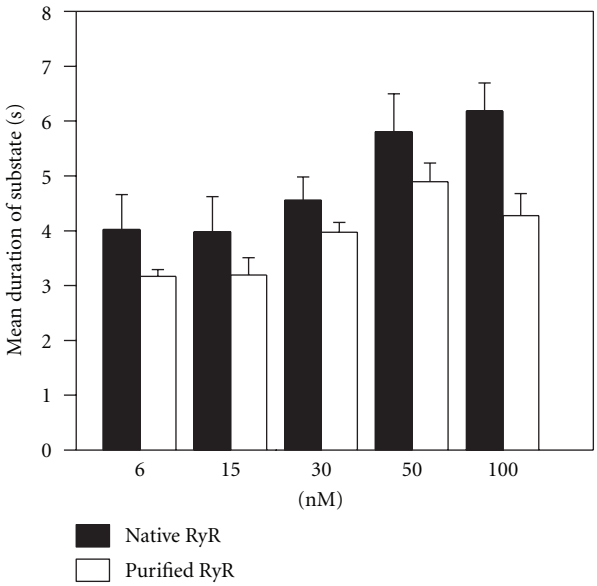

FIGURE 4: Effects of $IpTx_a$ on the mean durations of substate of native and purified RyR1. Mean durations of the substate events in native RyR1 versus purified RyR1 were determined in the presence of 6–100 nM $IpTx_a$. Data points are means ± SE for 10 experiments.

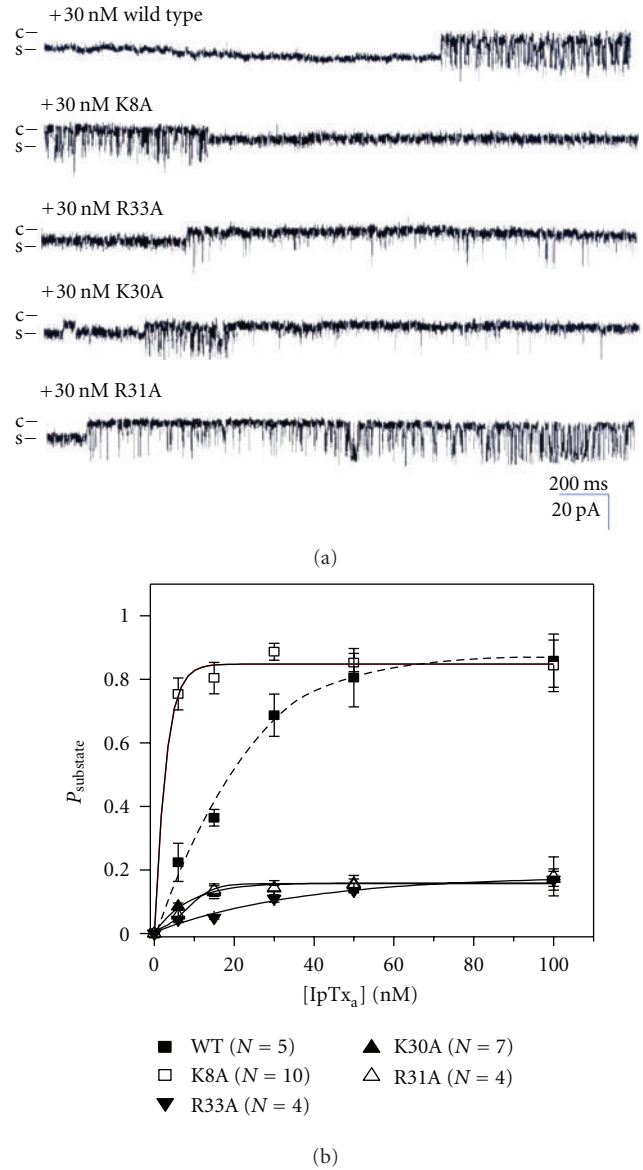

FIGURE 5: Properties of single channel gating in wild-type and mutant $IpTx_a$-modified purified RyR1. (a) Single channel currents of purified RyR1 activated in the presence of wild-type or mutant $IpTx_a$ were measured at −30 mV holding potential. The single channel opening is shown as a downward deflection. The recordings of single channel currents were measured at 30 nM wild-type or mutant $IpTx_a$ in the *cis* solution. (b) The plots of $P_{substate}$ of purified RyR1 versus wild-type or mutant $IpTx_a$ at various concentrations.

A to RyR1 was shown by [^{3}H]ryanodine binding and real-time Surface Plasmon resonance (SPR) studies. MCa and peptide A induced distinct modification of channel gating in an additive, but not competitive, manner. This indicates the possibility of an existence of independent binding sites for the two peptides on RyR1 [16]. These different results have been further understood by the hypothesis that the toxins and peptide A binding sites within RyR have both common activation site and independent substate sites [17]. Although the present results show that the mutations within the structural motif shared by Peptide A inhibited substate induction (Figure 2), it is hard to find direct evidence of competitive function in the common region of RyR1. Even though our investigations were undertaken without Peptide A, it could be suggested that the prolonged substate opening triggered by $IpTx_a$ is independent of the action of Peptide A [17]. Further study will be necessary to clarify whether the structurally conserved domains of $IpTx_a$ and Peptide A compete for the induction of substate in RyR1.

4.3. Comparison of the Active Sites with MCA. $IpTx_a$ and MCa share 82% aa identity in their primary structures. In addition to the similar β-sheet structure of the common stretch of the basic residues (Lys^{19}-Arg^{24}), the solution structures of $IpTx_a$ and MCa exhibit similar overall molecular folding [21, 30]. Because of this structural homology, these two toxins share functional similarities. Both $IpTx_a$ and MCa strongly induce SR Ca^{2+} release and activate ryanodine binding to skeletal RyR. In addition, both peptides have the ability to induce reversible transition of RyR1 gating mode between substate and fast full open gating [12, 13, 15–17]. Previously, it was demonstrated that mutations of each basic residue within Lys^{19}-Thr^{26} and mutation of Lys^8 of MCa decreased the ability of the toxin to induce Ca^{2+} release and potentiate [^{3}H]ryanodine binding in the SR [29]. Moreover, the occurrence of long-lasting substate was markedly prevented by mutations of the basic residues within Lys^{20}-Arg^{24} of MCa [29]. This inhibitory effect was reduced, if the mutation was farther from Lys^{24} while alanine replacement completely inhibited the substate event of skeletal RyR [17, 29]. Therefore, the previous results showing the effects of MCa mutants are partially coherent with our observations of the effects of $IpTx_a$ mutants on RyR1 substate. In the

Table 2: Effects of the mutant $IpTx_a$ on $P_{substate}$ of purified RyR1. $P_{substate,\ max}$ and EC_{50} for $P_{substate}$ of purified RyR1 were calculated as described in the legend to Table 1. Values are means ± SE of 4–10 experiments. The average lengths of the substate events were determined at 30 nM concentration. Asterisks indicate significant differences from the wild type for each parameter (Student t-test, $P < 0.05$). ND: not determined.

	$P_{substate}$		Mean duration of substate (s)
	$P_{substate,\ max}$	EC_{50} (nM)	
Wild type	0.86 ± 0.05	17.08 ± 2.31	3.97 ± 0.18
K8A	0.85 ± 0.02	5.29 ± 4.84*	ND
R33A	0.18 ± 0.06*	19.25 ± 1.05	1.43 ± 0.09*
K30A	0.16 ± 0.05*	15.66 ± 5.99	1.88 ± 0.22*
R31A	0.15 ± 0.02*	18.23 ± 1.65	3.15 ± 0.10*

present study, $IpTx_a$ mutant, R24A, was the most effective in decreasing mean duration of substate of RyR1 (Figure 3 and Table 1). R24A mutant showed comparable B_{max} value of $P_{substate}$ with those of other mutants, R23A, K22A, and K20A, although the values were significantly less than that of wild-type $IpTx_a$ (Figure 3 and Table 1). This suggests that the common domain clustered by positively charged residues (Lys^{20}-Arg^{24}) are responsible for the actions of two scorpion toxins to induce long-lasting substate opening of skeletal RyR1.

In spite of the high sequence identity, a significant functional difference between $IpTx_a$ and MCa has been observed. Two toxins induced different degree of substate of RyR1 at +40 mV holding potential (28% and 48% of full conductance state for $IpTx_a$ and MCa, resp.) [10, 13]. In addition, comparison of 3D structures of two peptides showed significantly different structural motifs near the N-terminal regions, where MCa but not $IpTx_a$ has a β-strand and makes the hydrophobic core by connecting to the side chains of four cysteine residues, Cys^{10}, Cys^{16}, Cys^{21}, and Cys^{32} [21]. Thus, the difference in the functional effect between $IpTx_a$ and MCa on RyR1 gating appears to be due to the subtle change in the local charge distribution or a structural dissimilarity. Here we further suggest and it appears that both acidic (e.g., Asp^2, Asp^{13}, and Glu^{29}) and basic residues of C-terminal region of $IpTx_a$ (e.g., Lys^{30}, Arg^{31}, and Arg^{33}) are involved in functional interaction with RyR1 in the case of $IpTx_a$ (Figure 2(b)). To our knowledge, to date there is no report regarding to the involvement of the acidic aa residues of $IpTx_a$ are related to the occurrence of $P_{substate}$ of RyR1.

5. Conclusions

In this study, the ability of charged aa residues of $IpTx_a$ to induce substate of RyR1 was examined in detail. Both basic and acidic aa residues are involved in producing substate of RyR1 supporting the hypothesis that the structural domain constituting a local cluster of charged aa is important for modifying the mode of channel gating [15, 16, 21]. Residues such as Lys^8 and Thr^{26} of $IpTX_a$ are important in terms of their inhibitory role in producing substate of RyR1. The modified channel gating properties induced by wild-type and mutant toxins were found both in native and purified RyR1. Taken together, the specific charge distributions on the surface of $IpTx_a$ may directly regulate the gating behavior of RyR1.

Acknowledgments

The authors thank Dr. M. Samso at Virginia Commonwealth University for providing the purified rabbit RyR1. This paper was supported by the Korea MEST NRF Grant (20110002144), the 2011 GIST Systems Biology Infrastructure Establishment Grant and KISTI-KREONET. I. R. Seo, D. E. Kang, and D. W. Song equally contributed to this paper.

References

[1] A. Tsugorka, E. Rios, and L. A. Blatter, "Imaging elementary events of calcium release in skeletal muscle cells," *Science*, vol. 269, no. 5231, pp. 1723–1726, 1995.

[2] E. Rios, J. Ma, and A. Gonzalez, "The mechanical hypothesis of excitation-contraction (EC) coupling in skeletal muscle," *Journal of Muscle Research and Cell Motility*, vol. 12, no. 2, pp. 127–135, 1991.

[3] W. Cheng, X. Altafaj, M. Ronjat, and R. Coronado, "Interaction between the dihydropyridine receptor Ca^{2+} channel β-subunit and ryanodine receptor type 1 strengthens excitation-contraction coupling," *Proceedings of the National Academy of Sciences of the United States of America*, vol. 102, no. 52, pp. 19225–19230, 2005.

[4] M. D. Stern and E. G. Lakatta, "Excitation-contraction coupling in the heart: the state of the question," *FASEB Journal*, vol. 6, no. 12, pp. 3092–3100, 1992.

[5] W. G. Wier, T. M. Egan, J. R. López-López, and C. W. Balke, "Local control of excitation-contraction coupling in rat heart cells," *Journal of Physiology*, vol. 474, no. 3, pp. 463–471, 1994.

[6] D. M. Bers, "Macromolecular complexes regulating cardiac ryanodine receptor function," *Journal of Molecular and Cellular Cardiology*, vol. 37, no. 2, pp. 417–429, 2004.

[7] J. J. Mackrill, "Ryanodine receptor calcium channels and their partners as drug targets," *Biochemical Pharmacology*, vol. 79, no. 11, pp. 1535–1543, 2010.

[8] D. W. Song, J. G. Lee, H. S. Youn, S. H. Eom, and D. H. Kim, "Ryanodine receptor assembly: a novel systems biology approach to 3D mapping," *Progress in Biophysics and Molecular Biology*, vol. 105, no. 3, pp. 145–161, 2011.

[9] R. El-Hayek, B. Antoniu, J. Wang, S. L. Hamilton, and N. Ikemoto, "Identification of calcium release-triggering and blocking regions of the II-III loop of the skeletal muscle dihydropyridine receptor," *The Journal of Biological Chemistry*, vol. 270, no. 38, pp. 22116–22118, 1995.

[10] Z. Fajloun, R. Kharrat, L. Chen et al., "Chemical synthesis and characterization of maurocalcine, a scorpion toxin that activates Ca^{2+} release channel/ryanodine receptors," *FEBS Letters*, vol. 469, no. 2-3, pp. 179–185, 2000.

[11] H. H. Valdivia, M. S. Kirby, W. J. Lederer, and R. Coronado, "Scorpion toxins targeted against the sarcoplasmic reticulum Ca^{2+}- release channel of skeletal and cardiac muscle," *Proceedings of the National Academy of Sciences of the United States of America*, vol. 89, no. 24, pp. 12185–12189, 1992.

[12] R. El-Hayek, A. J. Lokuta, C. Arevalo, and H. H. Valdivia, "Peptide probe of ryanodine receptor function: imperatoxin A, a peptide from the venom of the scorpion Pandinus imperator, selectively activates skeletal-type ryanodine receptor isoforms," *The Journal of Biological Chemistry*, vol. 270, no. 48, pp. 28696–28704, 1995.

[13] A. Tripathy, W. Resch, L. E. Xu, H. H. Valdivia, and G. Meissner, "Imperatoxin A induces subconductance states in Ca^{2+} release channels (ryanodine receptors) of cardiac and skeletal muscle," *Journal of General Physiology*, vol. 111, no. 5, pp. 679–690, 1998.

[14] A. Shtifman, C. W. Ward, J. Wang, H. H. Valdivia, and M. F. Schneider, "Effects of imperatoxin A on local sarcoplasmic reticulum Ca^{2+} release in frog skeletal muscle," *Biophysical Journal*, vol. 79, no. 2, pp. 814–827, 2000.

[15] G. B. Gurrola, C. Arévalo, R. Sreekumar, A. J. Lokuta, J. W. Walker, and H. H. Valdivia, "Activation of ryanodine receptors by imperatoxin A and a peptide segment of the II-III loop of the dihydropyridine receptor," *The Journal of Biological Chemistry*, vol. 274, no. 12, pp. 7879–7886, 1999.

[16] L. Chen, E. Estève, J. M. Sabatier et al., "Maurocalcine and peptide A stabilize distinct subconductance states of ryanodine receptor type 1, revealing a proportional gating mechanism," *The Journal of Biological Chemistry*, vol. 278, no. 18, pp. 16095–16106, 2003.

[17] A. F. Dulhunty, S. M. Curtis, S. Watson, L. Cengia, and M. G. Casarotto, "Multiple actions of imperatoxin A on ryanodine receptors: interactions with the II-III loop "A" fragment," *The Journal of Biological Chemistry*, vol. 279, no. 12, pp. 11853–11862, 2004.

[18] B. Lukacs, M. Sztretye, J. Almassy et al., "Charged surface area of maurocalcine determines its interaction with the skeletal ryanodine receptor," *Biophysical Journal*, vol. 95, no. 7, pp. 3497–3509, 2008.

[19] M. G. Casarotto, D. Green, S. M. Pace, S. M. Curtis, and A. F. Dulhunty, "Structural determinants for activation or inhibition of ryanodine receptors by basic residues in the dihydropyridine receptor II-III loop," *Biophysical Journal*, vol. 80, no. 6, pp. 2715–2726, 2001.

[20] R. El-Hayek and N. Ikemoto, "Identification of the minimum essential region in the II-III loop of the dihydropyridine receptor α1 subunit required for activation of skeletal muscle-type excitation-contraction coupling," *Biochemistry*, vol. 37, no. 19, pp. 7015–7020, 1998.

[21] C. W. Lee, E. H. Lee, K. Takeuchi et al., "Molecular basis of the high-affinity activation of type 1 ryanodine receptors by imperatoxin A," *Biochemical Journal*, vol. 377, no. 2, pp. 385–394, 2004.

[22] I. R. Seo, M. R. Choi, C. S. Park, and D. H. Kim, "Effects of recombinant imperatoxin A ($IpTx_a$) mutants on the rabbit ryanodine receptor," *Molecules and Cells*, vol. 22, no. 3, pp. 328–335, 2006.

[23] D. Green, S. Pace, S. M. Curtis et al., "The three-dimensional structural surface of two β-sheet scorpion toxins mimics that of an α-helical dihydropyridine receptor segment," *Biochemical Journal*, vol. 370, no. 2, pp. 517–527, 2003.

[24] D. H. Kim, S. T. Ohnishi, and N. Ikemoto, "Kinetic studies of calcium release from sarcoplasmic reticulum in vitro," *The Journal of Biological Chemistry*, vol. 258, no. 16, pp. 9662–9668, 1983.

[25] C. Miller and E. Racker, "Ca^{2+} induced fusion of fragmented sarcoplasmic reticulum with artificial planar bilayers," *Journal of Membrane Biology*, vol. 30, no. 1, pp. 283–300, 1976.

[26] J. S. Smith, R. Coronado, and G. Meissner, "Single channel measurements of the calcium release channel from skeletal muscle sarcoplasmic reticulum: activation by Ca^{2+} and ATP and modulation by Mg^{2+}," *Journal of General Physiology*, vol. 88, no. 5, pp. 573–588, 1986.

[27] E. H. Lee, G. Meissner, and D. H. Kim, "Effects of quercetin on single Ca^{2+} release channel behavior of skeletal muscle," *Biophysical Journal*, vol. 82, no. 3, pp. 1266–1277, 2002.

[28] F. A. Lai, H. P. Erickson, E. Rousseau, Q. Y. Liu, and G. Meissner, "Purification and reconstitution of the calcium release channel from skeletal muscle," *Nature*, vol. 331, no. 6154, pp. 315–319, 1988.

[29] E. Estève, S. Smida-Rezgui, S. Sarkozi et al., "Critical amino acid residues determine the binding affinity and the Ca^{2+} release efficacy of maurocalcine in skeletal muscle cells," *The Journal of Biological Chemistry*, vol. 278, no. 39, pp. 37822–37831, 2003.

[30] A. Mosbah, R. Kharrat, Z. Fajloun et al., "A new fold in the scorpion toxin family, associated with an activity on a ryanodine-sensitive calcium channel," *Proteins*, vol. 40, no. 3, pp. 436–442, 2000.